





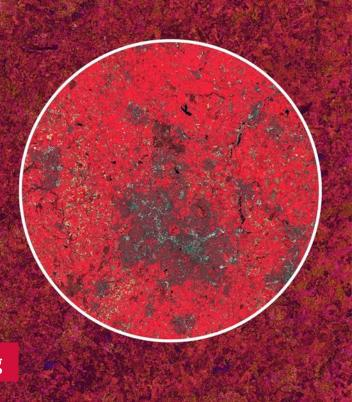
→ 8th ADVANCED TRAINING COURSE ON LAND REMOTE SENSING

10–14 September 2018
University of Leicester | United Kingdom

Urban Mapping

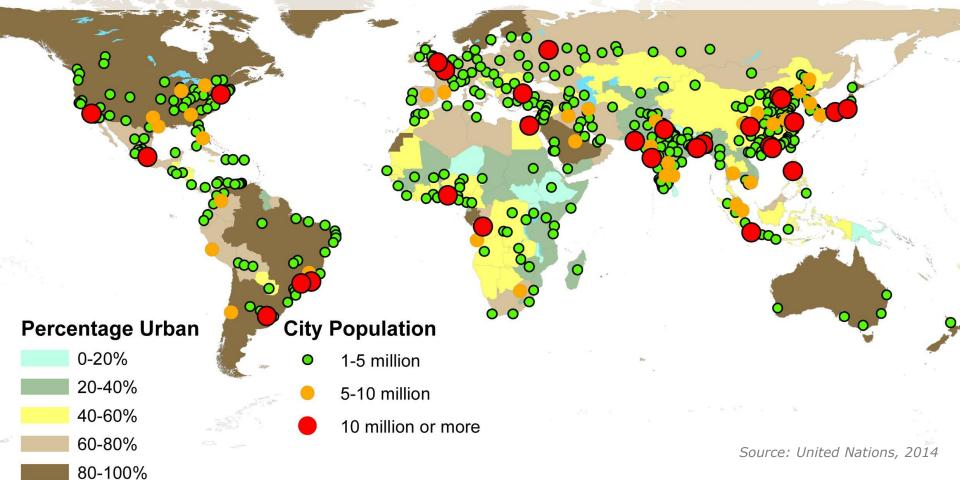
Sebastian van der Linden, Akpona Okujeni, Franz Schug

11/09/2018



Introduction to urban remote sensing

Introduction – The urban millennium





Urban areas from space

30x30 km footprint of Berlin, Germany, as seen by

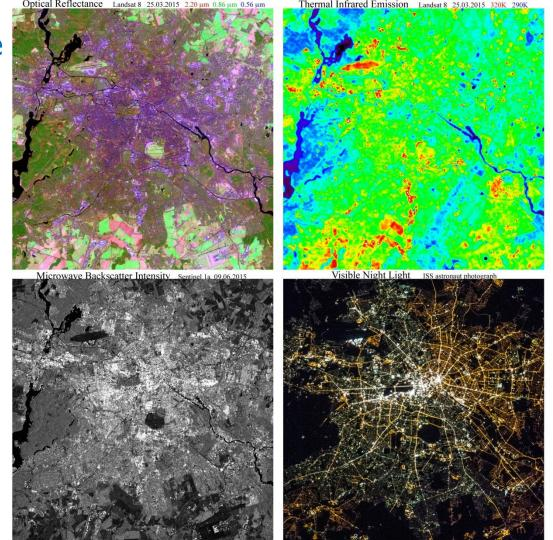
UL: Landsat 8 (swIR, nIR, red)

UR: Landsat 8 thermal

LL: Sentinel-1A

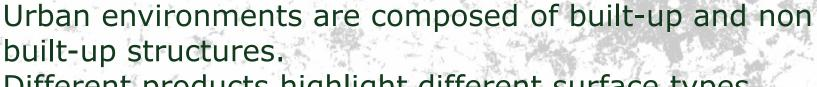
LR: vis. nightlights (ISS photo).

Each sensor system provides complementary information, but is also subject to non-uniqueness.



Source: Small et al., 2018

Global Urban Footprint: Berlin-Brandenburg TerraSAR-X product from DLR

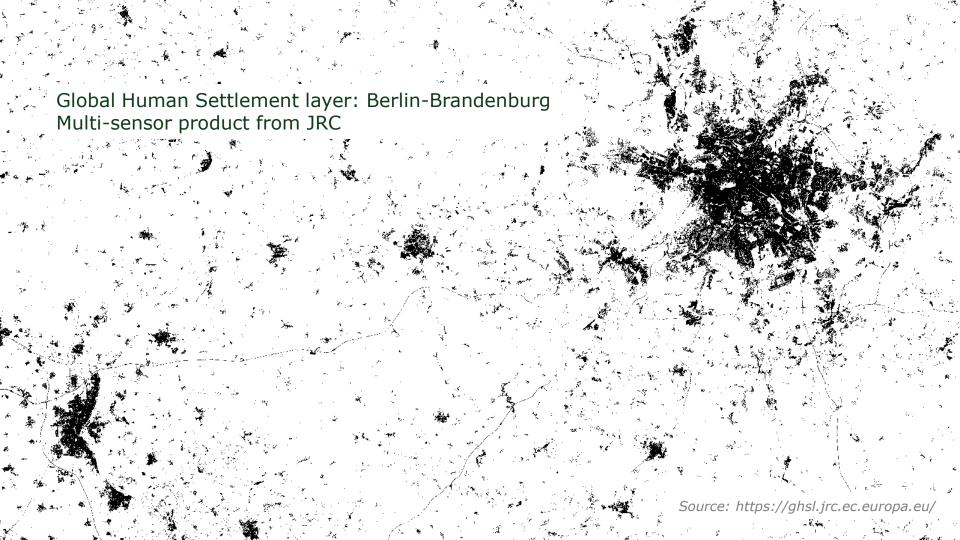


Different products highlight different surface types.

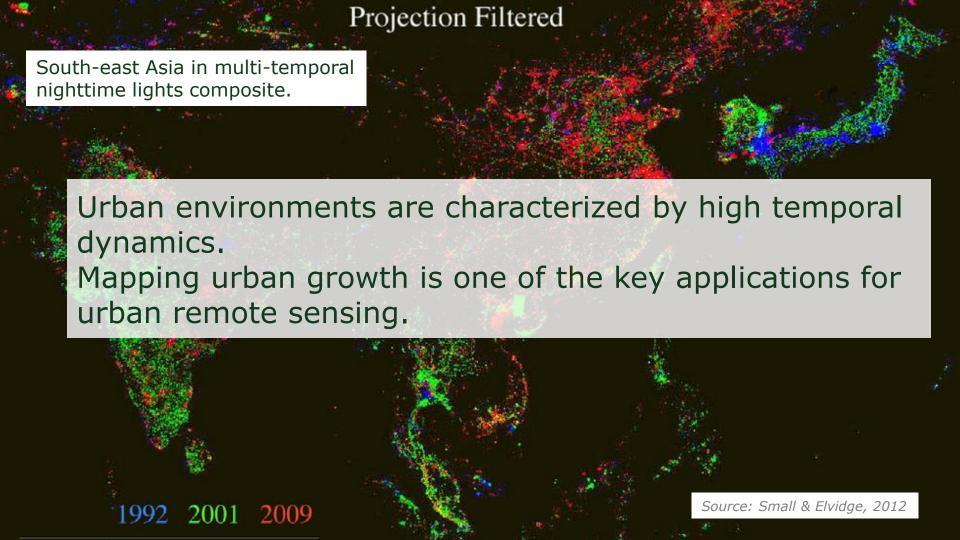
Source: www.dlr.de

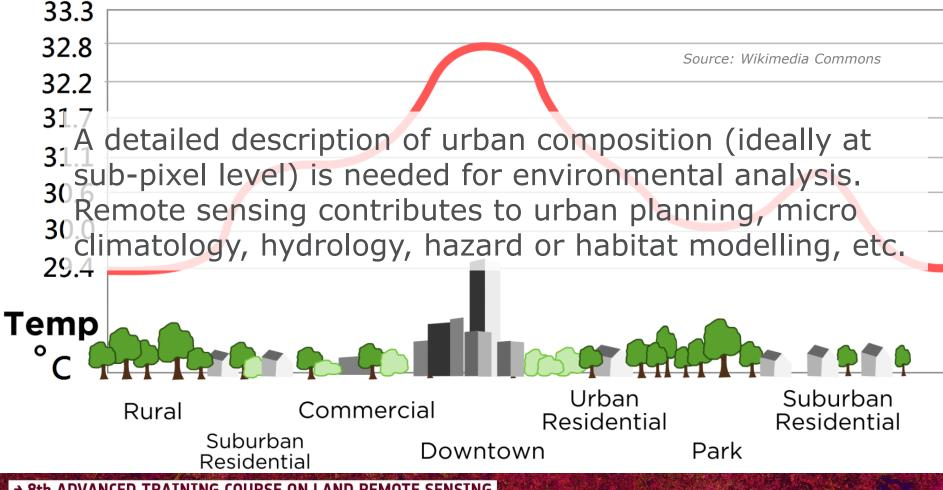
Global Urban Footprint: Berlin-Brandenburg TerraSAR-X product from DLR











Introduction (summary)

With more than have of the world's population living in cities and rapid urbanization rates, remote sensing plays a pivotal role in monitoring urban environments.

Especially in less developed countries and for fast growing urban agglomerations remote sensing is often the only reliable source of spatial information.

Most urban environmental models use remote sensing based maps as input.

Remote sensing analyses usually focus on

- mapping urban extent and growth
- mapping urban composition

Characteristics and challenges of urban remote sensing

Urban land cover

Urban land cover is characterized by great diversity of materials. Here the city of Berlin, Germany.







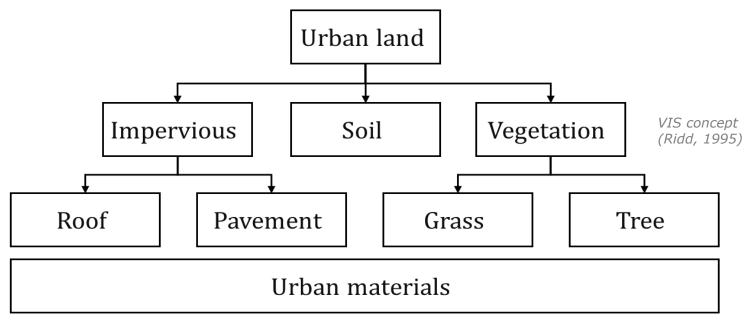




Source: Google Earth

Urban land cover

Urban land cover classes can be hierarchically organized down to the material level.



High **spectral**diversity of construction materials and natural surface types.

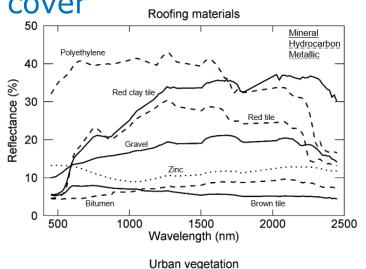
Over

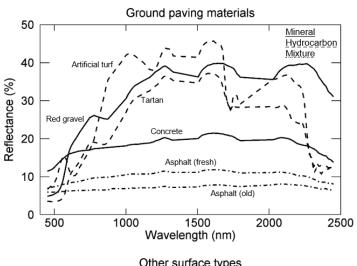
Folyethy

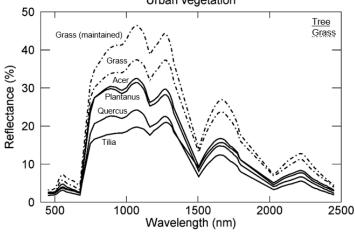
40
Polyethy

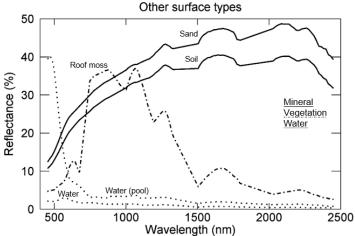
20
Polyethy

10









Source: Small et al., 2018

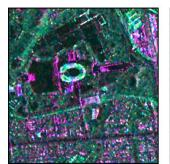
Urban land cover

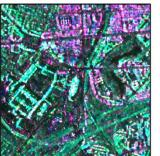
Polarimetric **SAR** representation of Berlin area and three subsets using TerraSAR-X StripMap data in the Pauli color coding scheme (R: HH-VV, G: HV, B: HH+VV).

Mirror-like reflectors appear dark (streets, sport fields, water). Vegetation is dark greenish with HV dominating. Strong backscatter structure appear bright, with the actual color (green to pink) also depending on object size, geometric arrangement and orientation.

Source: Small et al., 2018





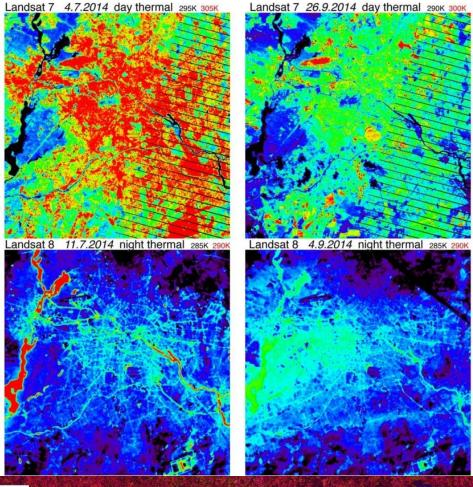




Urban land cover

Berlin area **thermal** emissions in July and September during day (top, Landsat-7) and night (bottom, Landsat-8).

Water bodies show low values at day and highest at night. Urban forests are always in mid-ranges. Street canyons and large buildings store energy longer and emit even at nighttime.



Source: Small et al., 2018

The factor scale in urban remote sensing

Step from approx. <1 m to 30 m leads to massive spatial aggregation.



HyMap 3.6 m 20.08.2009

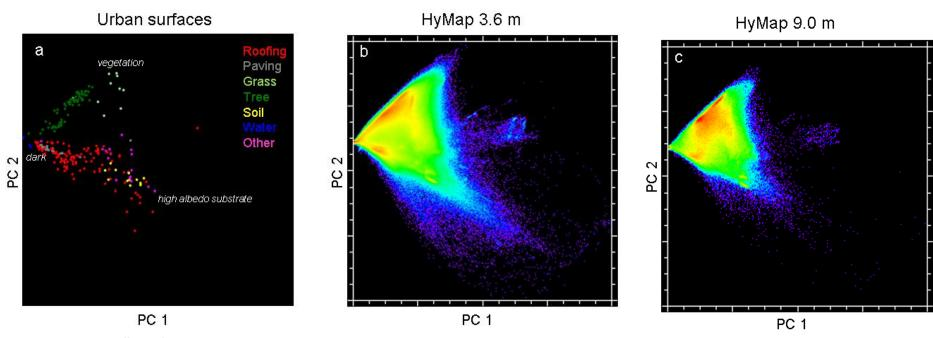


Sentinel-2 10 m 23.08.2015



The factor scale in urban remote sensing

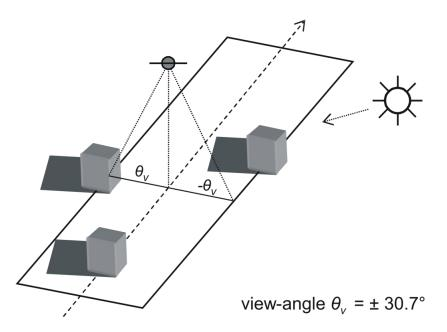
Step from approx. 5 m to 30 m leads to massive spectral aggregation.

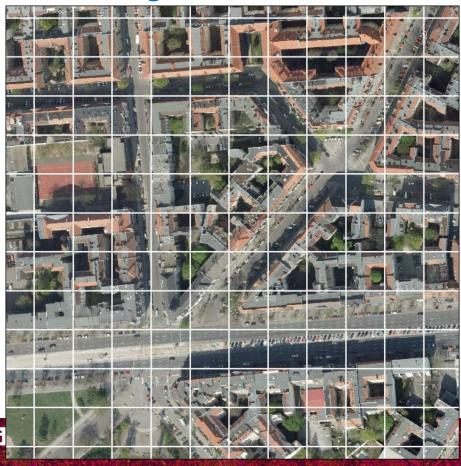


Source: Small et al., 2018

The factor scale in urban remote sensing

High number of mixed pixels. Complex 3-D geometry and illumination.





→ 8th ADVANCED TRAINING COURSE ON LAND REMOTE SENSING

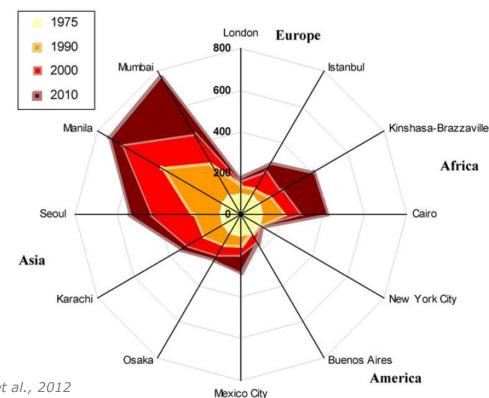
10-14 September 2018 | University of Leicester | United Kingdom

Mapping urban growth and urban composition

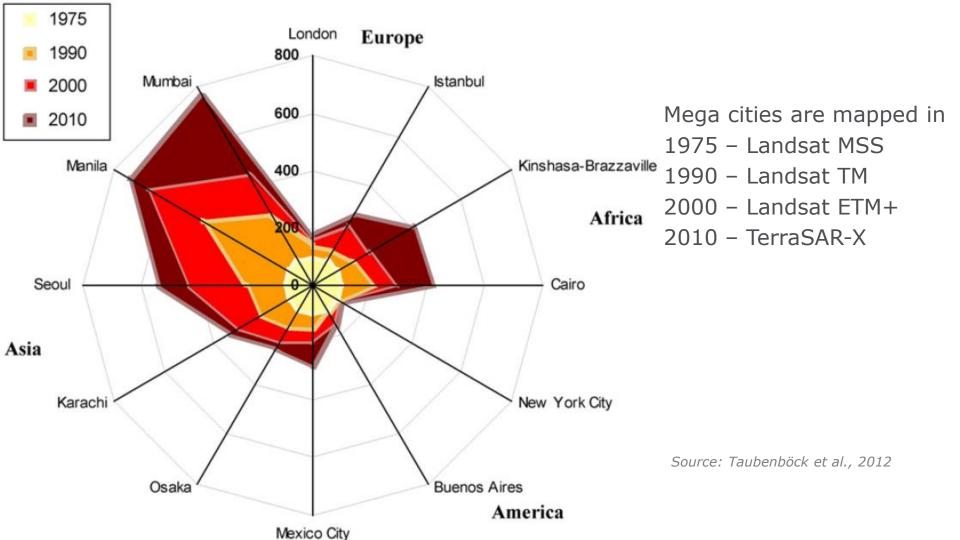
Mapping urban growth from optical and SAR data

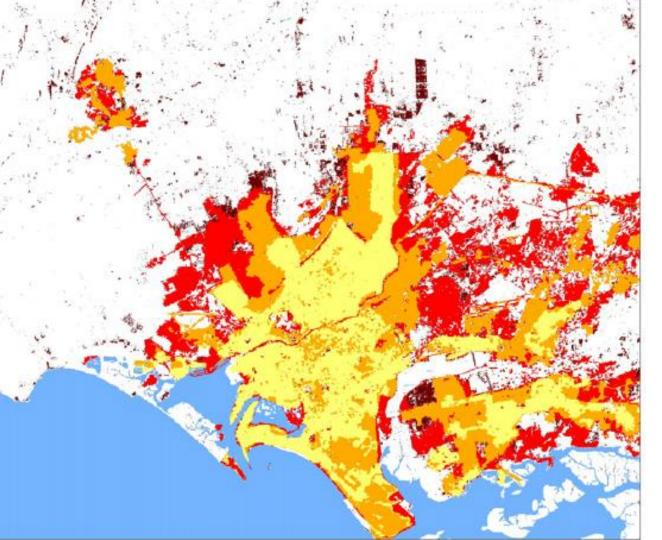
Urban growth can be mapped reliably by means of remote sensing.

Taubenböck et al. (2012) use data from TerraSAR-X and Landsat to quantify urban growth for global mega cities since 1975 in four time steps.



Source: Taubenböck et al., 2012





Map of Karachi, Pakistan



Source: Taubenböck et al., 2012

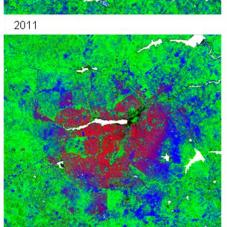
Mapping urban growth from optical data

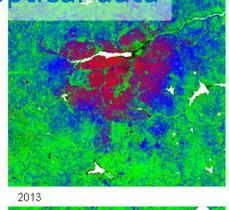
2002

Urban growth best described by sub-pixel fraction information, e.g. percent built-up cover.

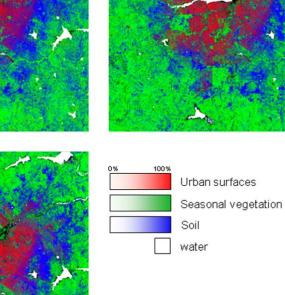
Spectral unmixing or regression analyses needed.

2011





2007



2009



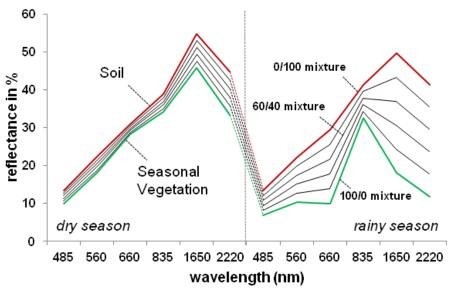
0 6 12 km

Source: Schug et al., 2018

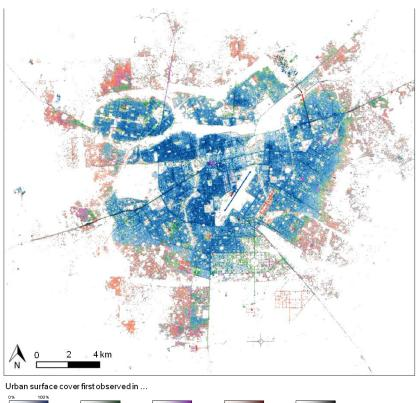
→ 8th ADVANCED TRAINING COURSE ON LAND REMOTE SENSING

Mapping urban growth from optical data

Information from two seasons allows reliable separation of soil and seasonal vegetation.

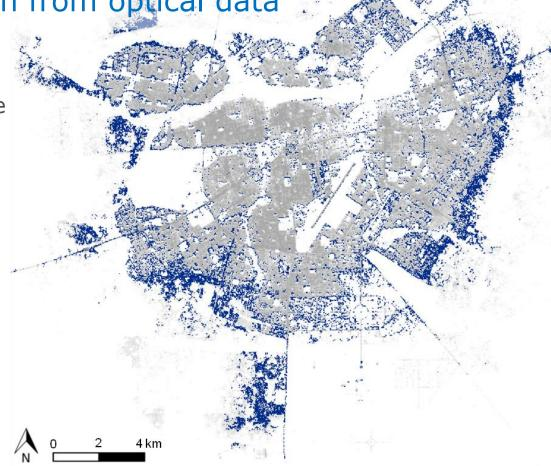


Source: Schug et al., 2018

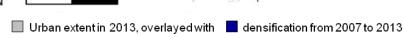


Mapping urban growth from optical data

Sub-pixel fraction allow the description of densification over time better than discrete classification results.

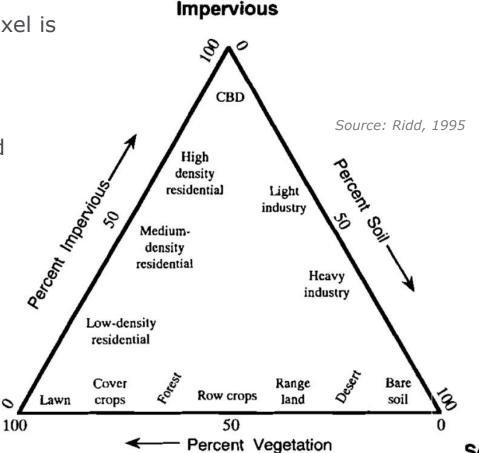


Source: Schug et al., 2018



Ridd (1995) assumes, every urban pixel is composed of impervious surface, vegetation or soil.

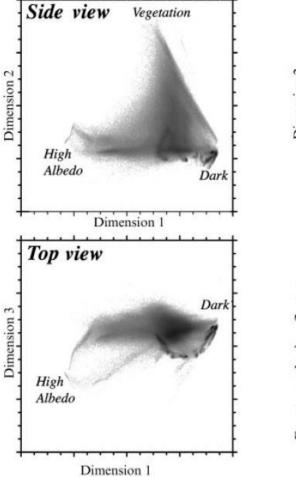
Ridd's V-I-S concept is based on a thematical framework. It is not based on the spectral characteristics of urban areas.



Vegetation

Soil

Small (2005) analysed more than 24 urban areas and concludes that the spectral properties working with Landsat ETM+ always relate to the degree of brightness and the portion of vegetation. This results in a mixing triangle in the first two PC components.

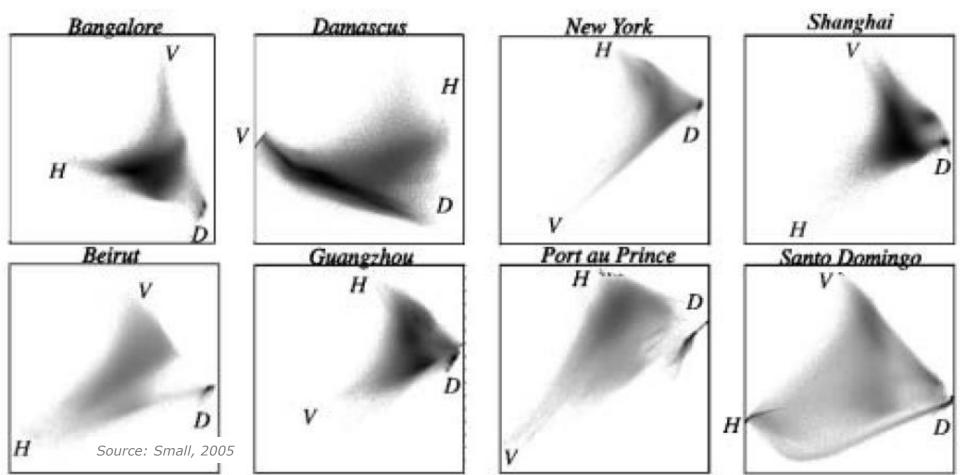


Dimension 2 Dimension 3 Exoatmospheric reflectance 0.6 0.8 1.0 1.2 1.4 1.6 1.8 2.0 2.2 Wavelength (um)

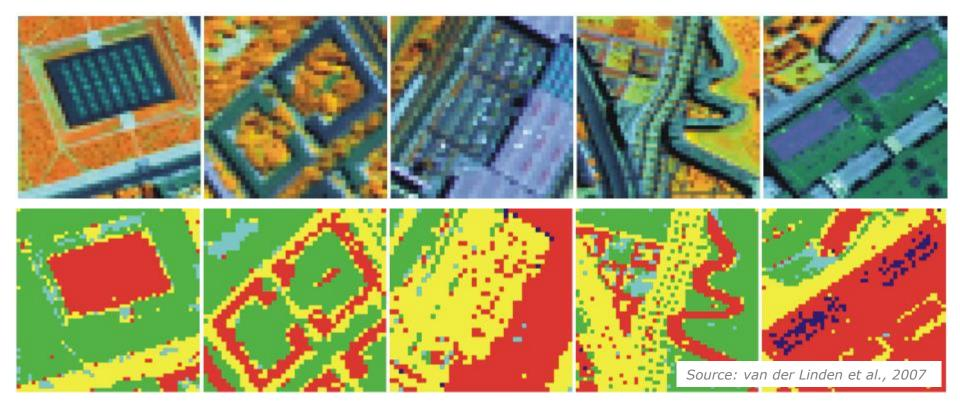
Vegetation

End view

Source: Small, 2005



Using higher spatial and spectral characteristics with machine learning more urban cover types can be mapped, as e.g. van der Linden et al. (2007) showed.



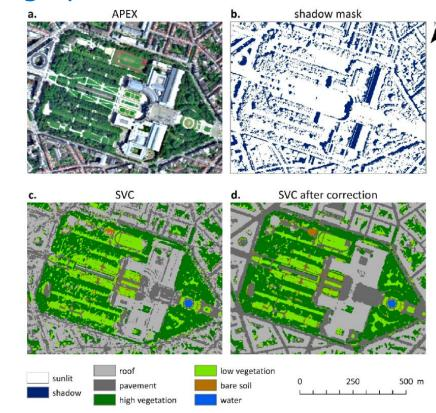
Mapping urban composition using spectral and lidar data

Land cover maps from APEX (2 m; 252 bands) and LiDAR data.

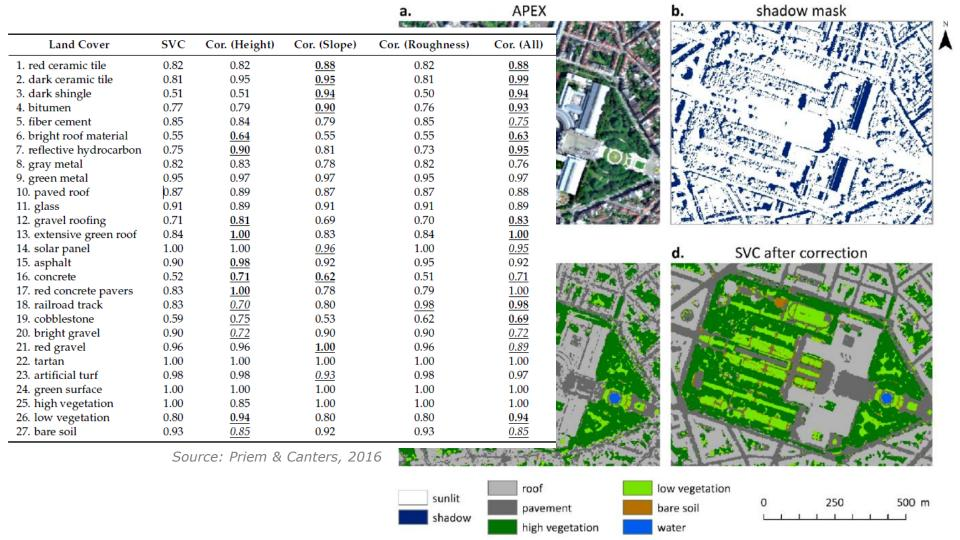
SVC classification with post-processing.

Height/shadow information to account for spectral ambiguity.

High share of pure pixels and high Accuracies.

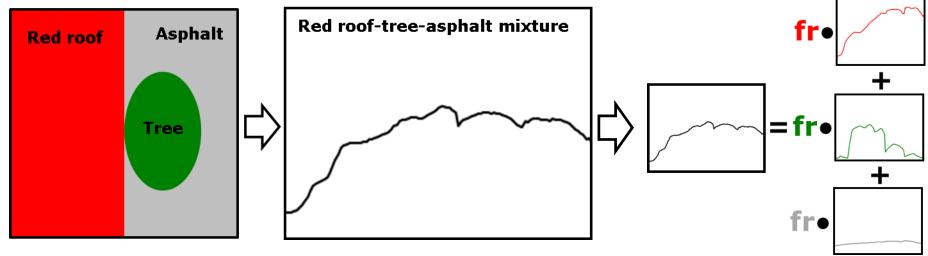


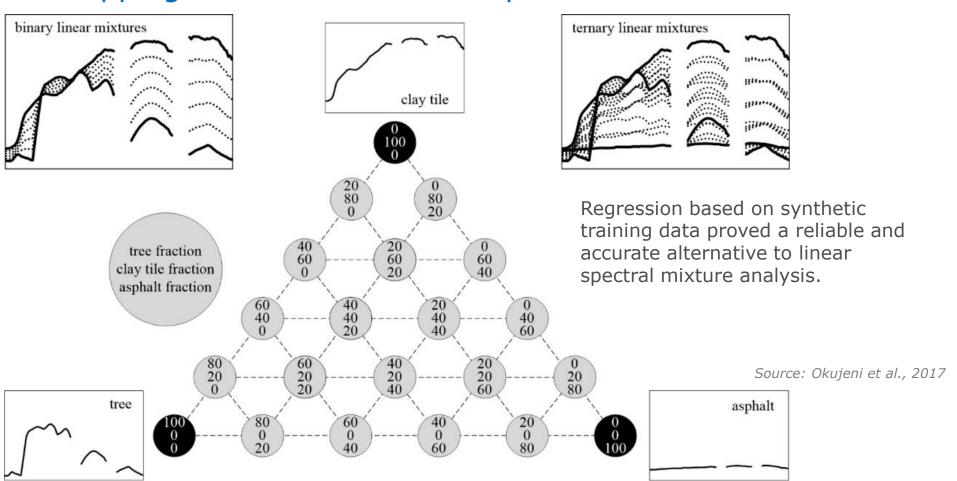
Source: Priem & Canters, 2016



Given the high number of mixed pixels in spaceborne data, fraction mapping appears more useful than classification to describe urban composition.

Concepts for quantitative mapping most often assume a linearly mixed spectrum, which can be decomposed into "pure" components, e.g. by linear spectral mixture analysis.

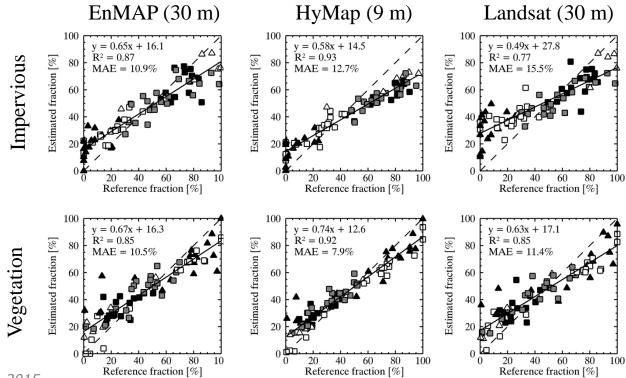




VIS components can be modelled at high accuracy using SVR with synthetic mixtures.

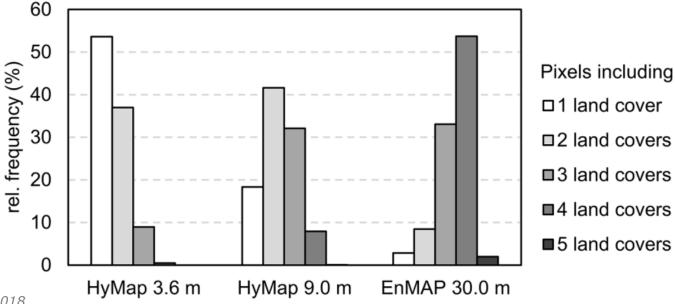
The decrease in accuracy from 9 m to 30 m is relatively low.

Hyperspectral EnMAP data leads to slightly better results than Landsat data.



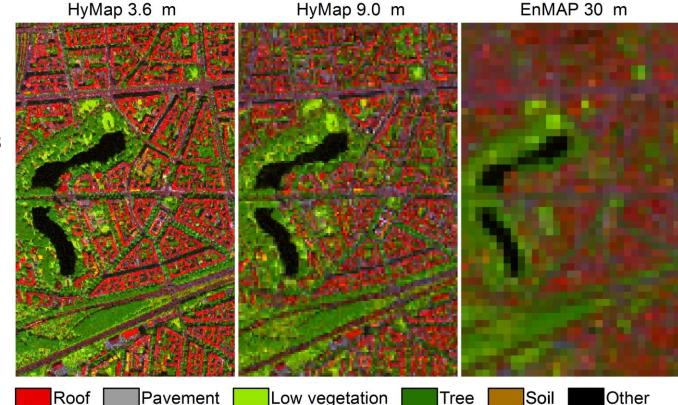
Source: Okujeni et al., 2015

The importance for sub-pixel analysis and mapping of fractions is illustrated by an analysis of frequency of extended VIS cover in image data at different resolutions.



Source: van der Linden et al., 2018

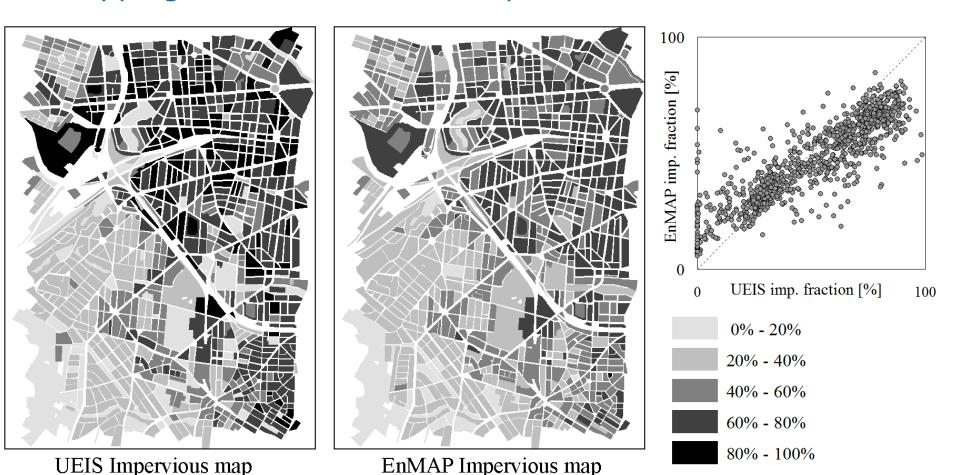
Accordingly, the number of mixed pixels increases at coarser resolutions, i.e. pure class colors appear mixed in fraction map.



EnMAP 30 m

Source: van der Linden et al., 2018

Low vegetation



Synthesis

Remote sensing of urban areas at high to very high resolutions is important.

Even at 10-20 resolutions a high number of mixed pixels prevails.

Quantitative maps of (sub-pixel) land cover fractions are needed to describe urban land surfaces with spaceborne remote sensing data.

Approaches for reliable and accurate fraction mapping are needed for urban remote sensing.

→ The practical will introduce you to regression-based mapping of urban areas!

References

Small, Okujeni, van der Linden, Waske (2018). In S. Liang: Comprehensive Remote Sensing.

Alonzo et al. (2014). Remote Sensing of Environment, 148, 70-83.

Griffiths et al. (2010). Remote Sensing of Environment, 114, 426-439.

van der Linden et al. (2007). Journal of Applied Remote Sensing, 1.

van der Linden et al. (2018). Surveys in Geophysics, DOI: 10.1007/s10712-018-9486-y.

Okujeni, van der Linden et al. (2013). Remote Sensing of Environment, 137, 184-197

Okujeni, van der Linden, Hostert (2015). Remote Sensing of Environment 108, 69-80.

Okujeni, van der Linden et al. (2017). J. of Selected Topics in Applied Remote Sensing, 10, 1640-1650.

Priem, Canters (2016). Remote Sensing, 8, 787

Ridd (1995). Int. Journal of Remote Sensing, 16, 2165-2185.

Small (2005). Int. Journal Remote Sens., 26, 661-681.

Small, Elvidge (2012). Int. Journal of Applied Earth Observation and Geoinformation. 22, 40-52.

Taubenböck et al. (2012). Remote Sensing of Environment, 117, 162-176.

United Nations (2014). World polulation prospects. https://esa.un.org/unpd/wpp/

Schug et al. (2018). Remote Sensing of Environment, 210, 217-228

If not indicated differently, figures are taken from the dissertations of S. van der Linden and A. Okujeni. See edoc.hu-berlin.de.

→ 8th ADVANCED TRAINING COURSE ON LAND REMOTE SENSING

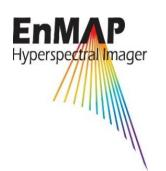
Thank you for your attention!

Geomatics Lab @ HU Berlin

Supported by:



on the basis of a decision by the German Bundestag









@HumboldtRemSens